J. Fluid Mech. (1992), *vol.* 240, *pp.* 659–679
Printed in Great Britain

Capillary rollers and bores

By MICHAEL S. LONGUET-HIGGINS
Institute for Nonlinear Science, University of California, San Diego, La Jolla, CA 92093-0402, USA

(Received 22 November 1991 and in revised form 17 January 1992)

At any free surface at which the tangential stress τ_{ns} vanishes there must be a surface vorticity $\omega = -2\kappa q$, where κ is the curvature and q the tangential velocity. In a surface wave on water, this condition produces a (Stokes) boundary layer with thickness of order $\delta = (2\nu/\sigma)^{\frac{1}{2}}$, where ν is the kinemetic viscosity and σ the radian frequency of the wave. To first order in the wave steepness parameter ak, the vorticity remains within the boundary layer, but at second order some escapes through the Stokes layer. The mean vorticity $\bar{\omega}$ at the outer edge of the Stokes layer is of order $2(ak)^2\sigma$, twice the mean vorticity generated at the free surface.

These results are applied to steep capillary waves, particularly the parasitic capillaries often seen on the forward face of short gravity waves. Because of the high value of σ for the capillaries, the vorticity they generate is much larger than that generated by the gravity wave itself. Hence the capillaries contribute significantly to the vortex (roller) often found at the crest of short gravity waves, when capillaries are present. It is argued that the crest roller and the capillaries form a cooperative system, a 'capillary roller' in which each supports the other, with the aid of surface tension and viscosity. Energy is supplied by the gravity wave.

A capillary roller is one instance of a more general phenomenon: a 'capillary bore', which is a noticeable feature of many disturbed water surfaces.

1. Introduction

A very intriguing phenomenon, which throws much light on the small-scale structure of the sea surface, is the occurrence of 'parasitic capillaries' on the forward face of moderately short gravity waves, especially those with wavelengths 5–50 cm; see figure 1 (*a*). These capillary waves were first studied experimentally by Cox (1958). Evidently their existence depends on the fact that a gravity wave and a much shorter capillary wave may have the same phase speed. The dynamical theory of the generation of parasitic capillaries has been developed by Longuet-Higgins (1963), Crapper (1970), Ruvinsky & Freidman (1981, 1985), and Ruvinsky, Feldstein & Freidman (1991). This so far takes into account only the first-order effects of viscous damping.

However, an important feature of short, steep gravity waves, especially those with parasitic capillaries, has been pointed out by Okuda, Kawai & Toba (1977) and also by Ebuchi, Kawamura & Toba (1987); see figure 1 (*b*). This is the occurrence of a very strong vortical region, or roller, at the crest of the gravity wave, even in the absence of wind (cf. Cox 1958). Similar effects can indeed be detected in small-scale capillary bores and from water jets entering a still-water surface (Koga 1982). The question arises: what is the source of this strong vorticity? The vorticity does not seem to be present in the trough of the gravity wave – only in the crest.

In the present paper we shall show that a very likely source of the crest vorticity

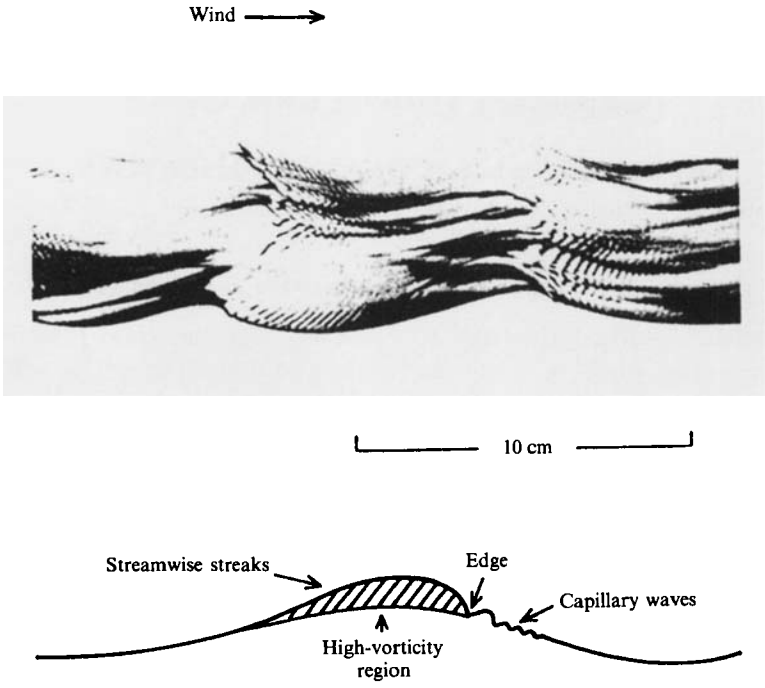

FIGURE 1. A close-up photograph of wind waves of length 9 cm taken with wind speed 6 m/s at fetch 6 m. Below is a schematic picture showing the high vorticity region at the gravity wave crests. (From Ebuchi *et al.* 1987.)

is the parasitic capillaries themselves, especially the steepest capillaries close to the forward edge of the roller. This is a nonlinear effect which can be understood in two steps. First, as proved in §2, we note that any *curved* free surface in a steady flow, irrotational or not, is necessarily a source of vorticity. The strength of the vorticity is $2\kappa q$, where κ is the curvature of the streamline at the surface and q is the stream velocity.

It follows that any oscillatory flow must develop a vortical boundary layer, or 'Stokes layer' (see §§4 and 5). To first order (§4), the vorticity diminishes exponentially inwards. But it is a remarkable fact that at second order, there is a mean 'rectified' vorticity just beyond the boundary layer. This must diffuse into the interior, in a similar way to the vorticity in the flow past a flat plate. For waves of small slope, the strength of this vorticity is double that generated at the surface itself, and is given by

$$\bar{\omega}_\infty = -2(ak)^2\sigma, \tag{1.1}$$

independently of the viscosity! Here, ak denotes the capillary wave steepness and σ the radian frequency. The simple result (1.1) has indeed been verified experimentally for gravity waves (Longuet-Higgins 1960). For capillary waves, however, the frequency σ is much higher than for gravity waves of the same phase speed. Hence the vorticity generated is much greater also. This vorticity from the capillaries accumulates mainly in the gravity wave crests.

The total vorticity diffused into the 'stream' which flows backwards under the ripples (in a frame of reference moving with the wave speed) is calculated in §6 below. It is found fully capable of producing a vortex beneath the crest of the gravity wave, with a velocity difference of order c (the phase-speed) between top and bottom of the vortex.

This conclusion is confirmed in §8 by an integral argument involving the mass transport in the capillary waves. Steep capillary waves have very rounded crests, in which the particle velocity almost equals the phase speed c. They are therefore propagated somewhat like 'balloons' of water floating on the undisturbed surface. When these waves are damped out by viscosity, their forwards momentum (mass transport) must be converted into a shearing current, in which the velocity difference between top and bottom is of order c.

For steep capillary waves having very sharply curved troughs, the surface vorticity may be shed into the interior differently, namely by flow separation below the wave troughs; see §9. Evidence of this effect, which can be accompanied by the trapping of air bubbles, is to be seen in the observations of Koga (1982).

The development of a capillary roller, from an initially irrotational wave, is discussed in §10. Conclusions and further suggestions follow in §11.

2. The vorticity generated at a free surface

In this section we prove some general results concerning the generation of vorticity.

Let (s, n) denote coordinates tangential and normal to any streamline in a steady, two-dimensional flow, as in figure 2. Here q denotes the particle speed and κ the curvature of the streamline – positive if the surface is concave. The tangential stress is denoted by τ_{ns}. Then we have:

THEOREM A. *In any steady flow in which the tangential stress vanishes, the vorticity at the surface must be given by*

$$\omega_s = -2\kappa q. \tag{2.1}$$

Proof. In general, if (u, v) are components of fluid velocity in the directions of any fixed rectangular coordinates (x, y) then

$$\omega = \frac{\partial v}{\partial x} - \frac{\partial u}{\partial y} \tag{2.2}$$

and

$$\tau_{ns} = \nu\left(\frac{\partial u}{\partial y} + \frac{\partial v}{\partial x}\right). \tag{2.3}$$

So if $\tau_{ns} = 0$, we have $\partial u/\partial y = -\partial v/\partial x$, hence

$$\omega = 2\frac{\partial v}{\partial x}. \tag{2.4}$$

Take the axes (x, y) tangential and normal to the streamline at a particular point O, and let θ be the angle between the tangents to the streamline at O and the general point P, as in figure 2. Then we have

$$v = -q\sin\theta \tag{2.5}$$

and

$$\frac{\partial}{\partial x} = \cos\theta\frac{\partial}{\partial s} + \sin\theta\frac{\partial}{\partial n}. \tag{2.6}$$

Performing the differentiation and setting $\theta = 0$ afterwards we get

$$\frac{\partial u}{\partial x} = -q\frac{\partial\theta}{\partial s} = -\kappa q, \tag{2.7}$$

since by definition $\kappa = \partial\theta/\partial s$. Substituting in equation (2.4) we obtain (2.1).

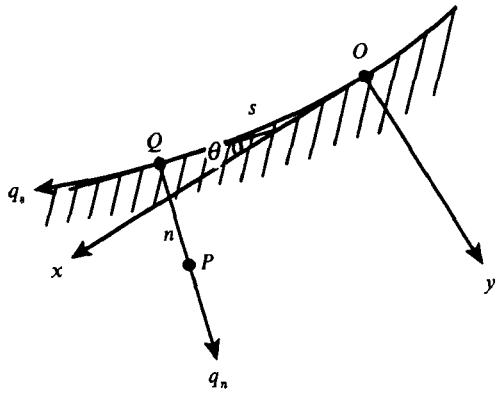

FIGURE 2. Definition of coordinates (s, n).

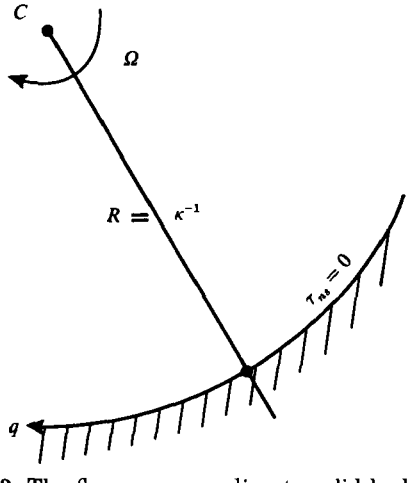

FIGURE 3. The flow corresponding to solid-body rotation.

Theorem A was derived less directly but in a more general form by Longuet-Higgins (1953; see equation (199)).

Physical interpretation. To ensure that $\tau_{ns} = 0$ the fluid must move locally so that there is no relative distortion of the fluid elements. That means that the local flow is a *solid rotation*, see figure 3. The particle speed q in this flow is given by

$$q = -\Omega r, \tag{2.8}$$

where Ω is the rate of rotation and r is the distance from the centre of rotation. Since r must be equal $1/\kappa$, where κ is the curvature, we have

$$\Omega = -\kappa q. \tag{2.9}$$

But it is well-known that the local rate of rotation Ω of a fluid element is just $\frac{1}{2}\omega$, where ω is the vorticity. Hence (2.9) is equivalent to (2.1).

Note that for any linearized surface wave, given by

$$y = a \cos ks \tag{2.10}$$

where y is the surface elevation and c the phase-speed, we have

$$\kappa = y_{xx} = -ak^2 \cos ks \tag{2.11}$$

and $q = -c$. Hence

$$\omega = -2\kappa q = ak\sigma \cos ks, \tag{2.12}$$

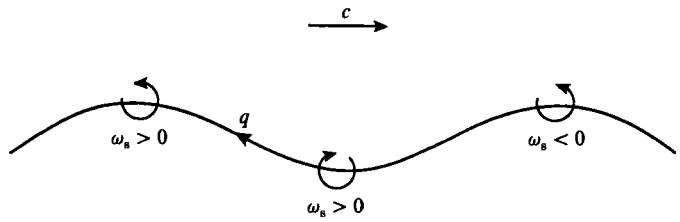

FIGURE 4. Schematic drawing of the vorticity in a progressive surface wave.

where $\sigma = ck$, the radian frequency. Thus ω is positive at the wave crests and negative in the wave troughs, as shown in figure 4.

A consequence of Theorem A is that in the absence of surface stresses, waves in real fluids cannot be entirely irrotational. Nevertheless, we can still use the well-known theory of irrotational waves as a first approximation, provided that we add boundary layers at the free surface (and if necessary at solid boundaries) to accommodate the non-zero values of the vorticity at the boundary (cf. Longuet-Higgins 1953, 1960). We shall now apply this procedure in the first place to pure capillary waves, that is waves so short that the influence of gravity on the phase speed can be considered as negligible.

3. Pure capillary waves

To illustrate the nonlinear behaviour of ω_s, we apply the results of §2 to Crapper's (1970) pure capillary wave solution, given in the form

$$z = \tan w - w, \tag{3.1}$$

where $z = x + \mathrm{i}y$, $w = \phi + \mathrm{i}\psi$ and we have chosen dimensionless units so that the phase speed c and wavenumber k are 1 and 2 respectively (see figure 5). Then it is easily found that

$$q = \left|\frac{\mathrm{d}z}{\mathrm{d}w}\right|^{-1} = \cot w \cot w^*, \tag{3.2}$$

where a star denotes the complex conjugate, and

$$\kappa = \frac{1}{2\mathrm{i}}\left(\frac{z_{ww}}{z_w} - \frac{z^*_{ww}}{z^*_w}\right) = \frac{\cos 2\phi \sinh 2\psi}{\sin^2 w \sin^2 w^*} \tag{3.3}$$

(see Longuet-Higgins 1988). The free surface may be chosen as any streamline $\psi = \psi_0$. The wave amplitude a (half the crest-to-trough height) is given by

$$ak = 2/\sinh 2\psi_0. \tag{3.4}$$

As can be verified, the free surface condition is satisfied, since

$$\tfrac{1}{2}q^2 + T\kappa = \tfrac{1}{2} \tag{3.5}$$

provided

$$\coth 2\psi_0 = 2T, \tag{3.6}$$

T being the surface tension in these units. Equation (3.6) serves as the dispersion relation.

A salient feature of the profiles in figure 5 is that as the wave amplitude increases, so the waves become more rounded in the crests and sharply curved in the troughs. In the limiting case $\psi_0 = 0.3941$ the ratio of the curvatures is about 50:1. Because of the relation (3.5), this implies that q is much greater in the troughs than in the crests.

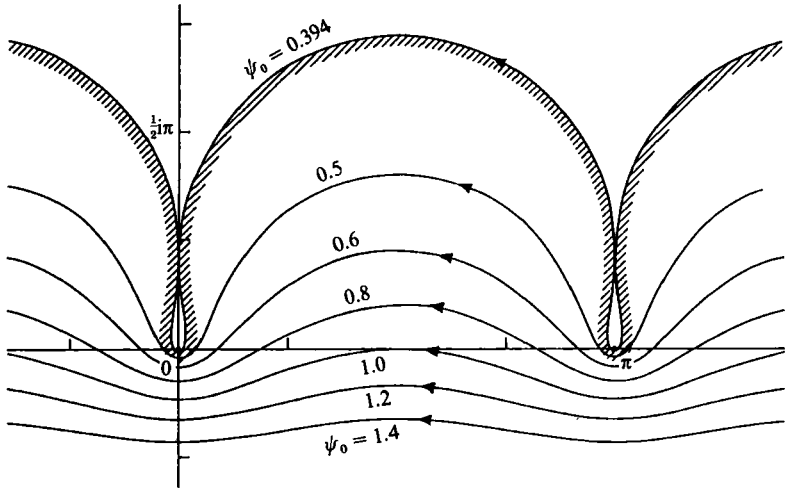

FIGURE 5. Streamlines and free surfaces in Crapper's solution for an irrotational, pure capillary wave, viewed in a frame of reference moving to the right with the phase speed c. Units are dimensionless, with $c = 1, k = 2$. (From Longuet-Higgins (1989.)

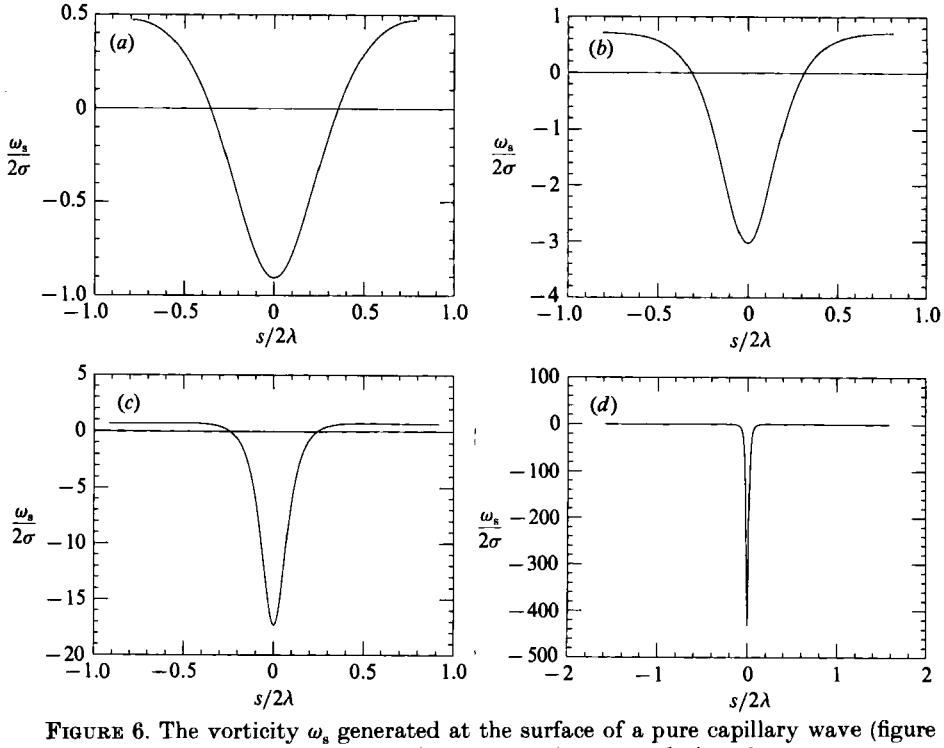

FIGURE 6. The vorticity ω_s generated at the surface of a pure capillary wave (figure 5): (a) $\psi_0 = 1.6$, (b) $\psi_0 = 1.2$, (c) $\psi_0 = 0.8$, (d) $\psi_0 = 0.4$.

In figure 6 we show the vorticity ω_s at the free surface as given by (2.12), plotted against the distance s along the free surface, $s = 0$ being taken in the wave trough. s may be calculated from

$$s = \int_0^\phi \frac{1}{q} \mathrm{d}\phi. \tag{3.7}$$

ψ_0	$2a/\lambda$	ak	$c/(Tk)^{\frac{1}{2}}$
1.6	0.0520	0.1633	0.9983
1.2	0.1165	0.3659	0.9918
0.8	0.2680	0.8419	0.9600
0.6	0.4218	1.3250	0.9130
0.5	0.5417	1.7018	0.8722
0.4	0.7168	2.2520	0.8149
0.3941	0.7298	2.2926	0.8108

TABLE 1. Parameters for pure capillary waves

Figures 6(*a*) to 6(*d*) show the cases $\psi_0 = 1.6$, 1.2, 0.8 and 0.4, corresponding to $ak = 0.163$ to 2.252 (see table 1). Even in case (*a*), that is for a fairly low wave steepness, it can be seen that ω_s is already quite nonlinear, being almost twice as great in the troughs as in the crests. As ψ_0 decreases to 0.4, the vorticity becomes almost entirely concentrated in the troughs, and elsewhere is relatively very small.

4. Boundary-layer theory: first approximation

We now develop a boundary-layer theory for viscous capillary–gravity waves which will be applicable, in the first place, only to waves of small or moderate steepness ak. The general trend of the results as the steepness increases will, however, be indicative of the results to be expected when ak is of order unity.

In any oscillatory flow, vorticity tends to diffuse inwards from the boundary on a lengthscale of order

$$\delta = (2\nu/\sigma)^{\frac{1}{2}}, \tag{4.1}$$

where ν is the kinematic viscosity and σ the radian frequency. Our approximation will be based on the assumption that

$$\gamma \equiv k\delta \ll 1, \tag{4.2}$$

where k is the wavenumber for the surface waves.

Some numerical values of γ are shown in table 2, in which we took $g = 981$ cm/s^2, $T = 75$ dyne/cm and $\nu = 0.013$ cm^2/s. For very small wavelengths ($k \gg 1$) γ varies only as $k^{\frac{1}{2}}$.

The profile of the free surface will be affected to order γ^2, not γ. For, the ratio of the viscous stress τ_{ns} to the normal stress τ_{nn} is of order

$$\frac{\tau_{ns}}{\tau_{nn}} \sim \frac{2\nu\kappa q}{T\kappa} = \frac{2\nu q}{T} \tag{4.3}$$

for capillary waves. But q is of the same order as the phase-speed c, that is $(Tk)^{\frac{1}{2}}$. Hence

$$\frac{\tau_{ns}}{\tau_{nn}} \sim \frac{2\nu c}{c^2/k} = \frac{2\nu k^2}{\sigma} = k^2\delta^2 = \gamma^2. \tag{4.4}$$

To first order in γ we may therefore use the inviscid streamlines as if they were the actual streamlines.

Let us write

$$(q_s, q_n) = (q_{s\mathrm{I}}, q_{n\mathrm{I}}) + (q_{s\mathrm{B}}, q_{n\mathrm{B}}), \tag{4.5}$$

where $(q_{s\mathrm{I}}, q_{n\mathrm{I}})$ are the tangential and normal components of velocity in the

λ (cm)	k $(\text{cm})^{-1}$	σ (s^{-1})	δ (mm)	γ
100	0.0628	7.85	0.575	0.0036
10	0.628	25.2	0.321	0.0202
1.74	3.617	84.2	0.176	0.0635
1.0	6.283	157.4	0.0129	0.0808
0.1	62.83	4320.0	0.0024	0.1541

TABLE 2. Values of the boundary-layer parameter γ

irrotational wave (seen in a frame of reference moving horizontally with the wave speed c) and $(q_{s\mathrm{B}}, q_{n\mathrm{B}})$ are velocity components of vortical flow induced by the diffusion of vorticity from the boundary.

$$q_{s\mathrm{I}}/c = O(1), \quad q_{s\mathrm{B}}/c = O(\gamma). \tag{4.6}$$

The equation of continuity can be written

$$\frac{\partial q_s}{\partial s} + \frac{\partial}{\partial n}(\eta q_n) = 0. \tag{4.7}$$

where $\eta = (1+n\kappa)$. So to lowest order in γ

$$q_n = \int_0^n -\frac{\partial q_s}{\partial s}\,\mathrm{d}n = -n\frac{\partial q_s}{\partial s}, \tag{4.8}$$

whence

$$q_{n\mathrm{I}} = -n\frac{\partial q_{s1}}{\partial s} = O(\gamma)\,c \tag{4.9}$$

and

$$q_{n\mathrm{B}} = -n\frac{\partial q_{s\mathrm{B}}}{\partial s} = O(\gamma^2)\,c. \tag{4.10}$$

Also the vorticity ω is given to lowest order by

$$\omega = \frac{\partial q_{s\mathrm{B}}}{\partial n} \tag{4.11}$$

so that

$$q_{s\mathrm{B}} = -\int \omega\,\mathrm{d}n. \tag{4.12}$$

Since in two-dimensional flow there is no stretching of the vortex lines, the basic equation for the vorticity is

$$\frac{\mathrm{D}\omega}{\mathrm{D}t} = \nu\nabla^2\omega, \tag{4.13}$$

where $\mathrm{D}/\mathrm{D}t$ denotes differentiation following the motion and ∇^2 is the two-dimensional Laplacian. In steady flow we thus have

$$\nu\nabla^2\omega = \left(q_s\frac{\partial}{\partial s} + q_n\frac{\partial}{\partial n}\right)\omega. \tag{4.14}$$

Within the boundary layer this reduces to

$$\nu\frac{\partial^2\omega}{\partial n^2} = \left(q_{s\mathrm{I}}\frac{\partial}{\partial s} + q_{n\mathrm{I}}\frac{\partial}{\partial n}\right)\omega. \tag{4.15}$$

Now let $\bar{q}$ denote the mean speed of a particle along the boundary, defined as

$$\bar{q} = \frac{1}{s_{\max}} \int_0^{s_{\max}} q_{sI}\, \mathrm{d}s. \tag{4.16}$$

Then we may write

$$\bar{q}_{sI} = \bar{q} + q'_{sI}, \tag{4.17}$$

where $\bar{q}'_{sI} = 0$, in an obvious notation. For low waves, $\bar{q}$ equals the phase speed c and q'_{sI} represents the tangential component of the orbital velocity. Then on substituting in (4.15) our basic vorticity equation becomes

$$\left(\nu \frac{\partial^2}{\partial n^2} - \bar{q} \frac{\partial}{\partial s}\right)\omega = q'_{sI} \frac{\partial \omega}{\partial s} - n \frac{\partial q'_{sI}}{\partial s} \frac{\partial \omega}{\partial n}. \tag{4.18}$$

The boundary condition at $n = 0$ is that

$$\omega = -2\kappa q_{sI} = -2\kappa(\bar{q} + q'_{sI}) \quad \text{when} \quad n = 0. \tag{4.19}$$

Also

$$\nabla\omega \to 0 \quad \text{as} \quad n \to \infty. \tag{4.20}$$

To solve these equations we now make a perturbation expansion in powers of an ordering parameter ϵ. Thus we set

$$q'_{sI} = \epsilon q_{sI1} + \epsilon^2 q_{sI2} + \dots, \tag{4.21}$$

$$\kappa = \epsilon \kappa_1; \tag{4.22}$$

we absorb all higher powers of ϵ into κ_1. It will be noted that $\bar{q}_{sI1} = \bar{q}_{sI2} = 0$. Also, since $\kappa = \partial\theta/\partial s$, where θ is periodic,

$$\bar{\kappa}_1 = 0. \tag{4.23}$$

We then seek a solution for ω in the form

$$\omega = \epsilon\omega_1 + \epsilon^2\omega_2 + \dots \tag{4.24}$$

by successive approximation.

On substituting in equations (4.18)–(4.20) and equating the coefficients of ϵ we have

$$\left(\nu \frac{\partial^2}{\partial n^2} - \bar{q} \frac{\partial}{\partial s}\right)\omega_1 = 0, \tag{4.25}$$

$$\omega_1 = -2\kappa_1 q \quad \text{when} \quad n = 0, \tag{4.26}$$

$$\frac{\partial w_1}{\partial n} \to 0 \quad \text{when} \quad n \to \infty. \tag{4.27}$$

Suppose now that κ_1 is given as a Fourier series in s:

$$\kappa_1 = \sum_{l=1}^{\infty} C_l \mathrm{e}^{\mathrm{i}lKs}, \quad K = 2\pi/s_{\max}; \tag{4.28}$$

equations (4.22) have the unique solution

$$\omega_1 = -2\bar{q} \sum_{l=1}^{\infty} C_l \mathrm{e}^{\mathrm{i}lKs - l^{\frac{1}{2}}\alpha n}, \tag{4.29}$$

where

$$\alpha^2 = \mathrm{i}\sigma/\nu, \quad R(\alpha) > 0 \tag{4.30}$$

so

$$\alpha = \frac{1+\mathrm{i}}{\delta}. \tag{4.31}$$

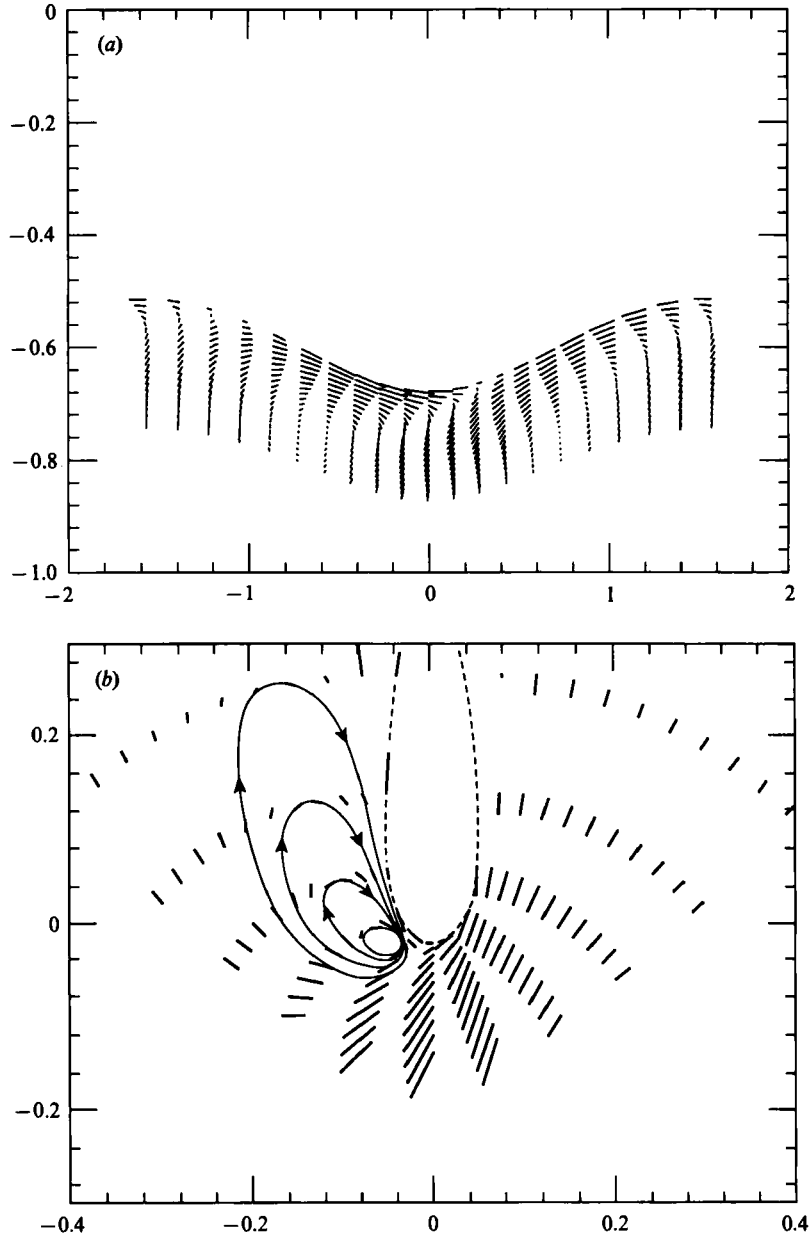

FIGURE 7. The first-order flow (q_{sB1}, q_{nB1}) in the boundary layer for the capillary waves in figure 6: (*a*) $\psi_0 = 1.6$, (*b*) $\psi_0 = 0.4$.

Each term on the right of (4.26) represents a term decaying inwards exponentially, but with a complex exponent α. The corresponding velocity components are calculated from

$$q_{sB1} = \int_n^\infty \omega_1 \, \mathrm{d}n \tag{4.32}$$

and from equation (4.15) respectively. A typical example is shown in figure 7 (*a*). The tangential component q_{sB1} tends to be greatest, and in the direction of propagation,

at a point lagging 45° behind the wave trough. There is an eddy, due to the varying normal velocity $q_{n\mathrm{B1}}$, with centre approximately 90° behind the trough. For the very steep wave shown in figure 7(*b*), there features are shifted closer to the trough.

In this first approximation the vorticity ω is confined to the Stokes boundary layer, and none escapes beyond a distance of order δ. In the next approximation we shall see that the situation is quite different.

5. The mean vorticity

By Theorem A, the mean vorticity $\bar{\omega}_s$ at the free surface is given by

$$\bar{\omega}_s = -2\overline{\kappa q} = -2\overline{\kappa_1 q'_{s1}} \tag{5.1}$$

since $\bar{\kappa} = \overline{\partial\theta/\partial s} = 0$ by the periodicity. Now for any sinusoidal wave such as (2.10) in deep water we have

$$q'_{s11} = -a\sigma\cos ks, \tag{5.2}$$

where $\sigma = kc$ is the radian frequency. Thus the tangential velocity q'_{s11} correlates with the curvature κ_1, and from (2.11) and (5.1) we find

$$\bar{\omega}_s = -(ak)^2\sigma, \tag{5.3}$$

when ak is small. In other words, the mean vorticity is negative. We show in figure 8 the value of $-\bar{\omega}_s$ for the finite-amplitude capillary waves of figure 5, plotted against $(ak)^2$. It can be seen that this increases like $(ak)^2$ at first, but then less rapidly.

We shall now prove a remarkable result, derived in more general form in Longuet-Higgins (1953), but here proved more simply:

THEOREM B. *In a progressive wave, when the tangential stress at the surface vanishes, the mean vorticity $\bar{\omega}_\infty$ just beyond the Stokes layer is just double the mean vorticity $\bar{\omega}_s$ at the free surface.*

Proof. Taking averages with respect to S in equations (4.18)–(4.20) we have, to order ϵ^2,

$$\nu\frac{\partial^2\bar{\omega}}{\partial n^2} = \overline{q'_{s1}\frac{\partial\omega}{\partial s}} - \overline{\frac{\partial q_{s1}}{\partial s}n\frac{\partial\omega}{\partial n}}, \tag{5.4}$$

$$\bar{\omega} = -2\overline{\kappa q_{s1}} \quad \text{when} \quad n = 0, \tag{5.5}$$

$$\frac{\partial\bar{\omega}}{\partial n} \to 0 \quad \text{when} \quad n \to \infty \tag{5.6}$$

(for clarity, the suffices 1 and 2 are omitted). Now in any two periodic quantities A and B we have $\overline{\partial A/\partial s\, B} = \overline{A\,\partial B/\partial s}$. Hence

$$\begin{aligned}\nu\frac{\partial^2\bar{\omega}}{\partial n^2} &= \overline{q'_{s1}\frac{\partial\omega}{\partial s}} + \overline{q'_{s1}n\frac{\partial^2\omega}{\partial s\partial n}} \\ &= \frac{\partial}{\partial n}\overline{\left(q'_{s1}n\frac{\partial\omega}{\partial s}\right)} \\ &= \overline{\frac{\partial q_{s1}}{\partial n}q'_{s1}n\frac{\nu}{c}\frac{\partial^2\omega}{\partial n^2}}\end{aligned} \tag{5.7}$$

by (4.15). Integrating from $n = \infty$, where both $\partial\bar{\omega}/\partial n$ and $\partial\omega/\partial n$ vanish, we have

$$\frac{\partial\bar{\omega}}{\partial n} = \overline{q'_{s1}n\frac{\partial^2\omega}{\partial n^2}}\Big/\bar{q}. \tag{5.8}$$

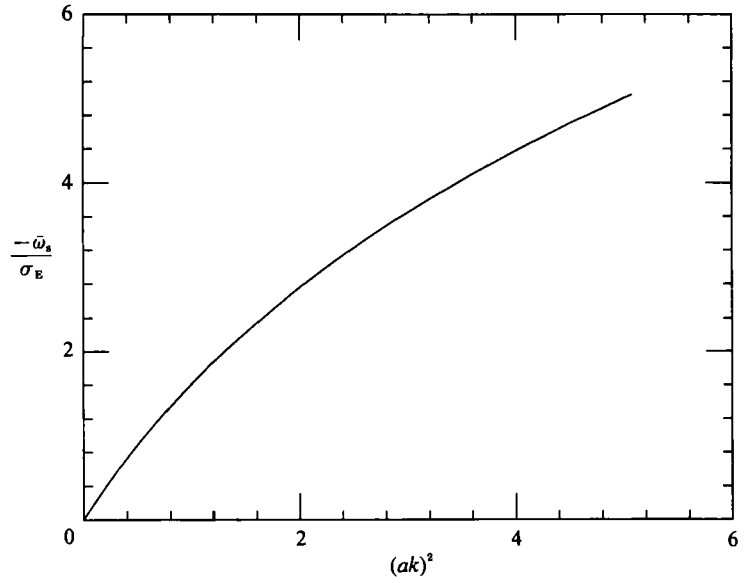

FIGURE 8. The mean vorticity $\bar{\omega}_s = -2\bar{\kappa}\bar{q}$ generated at the surface of the pure capillary wave of figure 5, as a function of $(ak)^2$.

A second integration from $n = 0$ gives

$$\bar{\omega} - \bar{\omega}_s = \overline{q'_{sI}\left(n\frac{\partial\omega}{\partial n} - \omega + \omega_0\right)}\Big/\bar{q} \tag{5.9}$$

where a suffix zero denotes the values at $n = 0$. Letting $n \to \infty$ we find

$$\begin{aligned}\bar{\omega}_\infty - \bar{\omega}_s &= \overline{q'_{sI}\,\omega_0}/\bar{q} \\ &= \overline{q'_{sI}(-2\kappa\bar{q})}/\bar{q} \\ &= -2\overline{\kappa q'_{sI}} \\ &= \bar{\omega}_s. \end{aligned} \tag{5.10}$$

Thus
$$\bar{\omega}_\infty = 2\bar{\omega}_s, \tag{5.11}$$

the result to be proved.

From (5.3) it follows that for low waves

$$\bar{\omega}_\infty = -2(ak)^2\sigma \tag{5.12}$$

independently of the viscosity or of the dispersion relation.

This result has been checked experimentally for low gravity waves of periods of 0.65 to 1.2 s, see Longuet-Higgins (1960). The demonstration depended on a further remarkable result:

THEOREM C. *For low waves, the mean shear due to the vorticity shed from beneath the Stokes boundary layer exactly doubles the shear due to the irrotational mass-transport velocity.*

For, the mean shear due to the vorticity (5.12) is

$$\left(\frac{\partial \bar{u}}{\partial y}\right)_{\text{vort}} = 2(ak)^2 \sigma. \tag{5.13}$$

On the other hand the irrotational mass-transport velocity

$$U = a^2 \sigma k \, \mathrm{e}^{2ky} \tag{5.14}$$

induces a shear

$$\frac{\partial U}{\partial y} = 2(ak)^2 \sigma \, \mathrm{e}^{2ky}, \tag{5.15}$$

which when $y = 0$ is precisely equal to (5.13). Together, the observed shear beneath the Stokes layer becomes

$$\left(\frac{\partial \bar{u}}{\partial y}\right)_{\text{tot}} = 4(ak)^2 \sigma. \tag{5.16}$$

This was the value observed.

6. Diffusion of the mean vorticity

Unlike the periodic components, the mean vorticity $\bar{\omega}_\infty$ will diffuse into the interior of the fluid on a longer timescale than the wave period, according to the diffusion equation

$$\frac{\partial \bar{\omega}}{\partial t} = \nu \frac{\partial^2 \bar{\omega}}{\partial n^2}. \tag{6.1}$$

When n becomes comparable with k^{-1}, it may be replaced by z, the mean depth of a particle below the mean surface level. On this time- and lengthscale, if $t = 0$ is the time at which the motion is started, we find from (6.1) that

$$\bar{\omega}(z, t) = \frac{2\bar{\omega}_\infty}{\pi^{\frac{1}{2}}} \int_Z^\infty \mathrm{e}^{-\lambda^2} \mathrm{d}\lambda, \tag{6.2}$$

where

$$Z = z/2(\nu t)^{\frac{1}{2}}. \tag{6.3}$$

The horizontal velocity $\bar{u}$ associated with this vorticity is given by

$$\bar{u} = \int_z^\infty \bar{\omega}(z, t) \, \mathrm{d}z, \tag{6.4}$$

that is

$$\bar{u} = \frac{4}{\pi^{\frac{1}{2}}} (\nu t)^{\frac{1}{2}} \bar{\omega}_\infty \left[\tfrac{1}{2}\mathrm{e}^{-Z^2} - Z \int_Z^\infty \mathrm{e}^{-\lambda^2} \mathrm{d}\lambda\right]. \tag{6.5}$$

In particular at the mean surface level $z = 0$ we have

$$\bar{u}_0 = -\frac{2}{\pi^{\frac{1}{2}}} (\nu t)^{\frac{1}{2}} \bar{\omega}_\infty. \tag{6.6}$$

This can also be written

$$\bar{u}_0 = -2N^{\frac{1}{2}} \delta \bar{\omega}_\infty, \tag{6.7}$$

where $N = \sigma t/2\pi$ is the number of wave cycles after starting the motion and δ is the boundary-layer thickness, defined by (4.1). A graph of $\bar{u}$ as a function of k_z after N cycles is shown in figure 9, for various values of N.

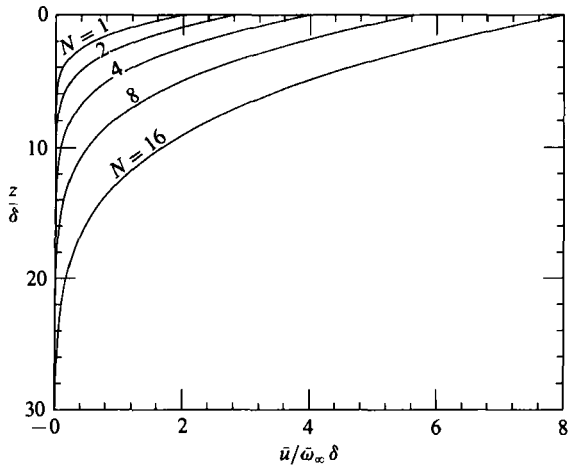

FIGURE 9. The mean horizontal velocity $\bar{u}$ after N cycles, shown as a function of the mean depth z.

7. Capillary rollers

As seen in figure 1, a finite train of capillary waves often forms just ahead of the crest of a short gravity wave on which there is a strong 'roller', or concentration of vorticity. In a frame of reference moving with the phase speed c, the particles at the surface of the crest travel slightly forwards whereas the particles beneath the roller travel backwards with nearly the phase speed. Thus there is in the roller itself a strong negative vorticity. This strong shearing flow appears also to produce three-dimensional instabilities in the form of vortices having axes aligned in the direction of wave propagation, similar to a Langmuir circulation. We regard the latter as a secondary, though important, effect, but enquire here only into the source of the primary, two-dimensional vorticity.

We remark that the rollers associated with parasitic capillaries are but one example of a more general class of flows which we may call 'capillary bores'; see figure 10. A *capillary bore* may be defined as a small jump in surface elevation, where the surface may be locally vertical, ahead of which is a train of short capillary waves, and behind which is found a strong negative vortex. Such flows are seen frequently on a disturbed water surface, with or without the presence of wind, and they occur on a range of scales. Generally the smaller scales appear to be laminar, the larger scales turbulent. The model we propose assumes that the flow is laminar.

We shall first estimate the total amount of the vorticity shed by a finite train of capillary waves. Separation of the flow will not be assumed. In §§3–6 above we neglected the decay of the wave train with horizontal distance x in the direction of wave propagation. For a uniform wave train the time-rate of decay of the amplitude a is given by

$$\frac{1}{a}\frac{\partial a}{\partial t} = -2\nu k^2 \tag{7.1}$$

(see Lamb 1932, p. 348). In a capillary roller, however, the source of the capillary wave energy is localized near the gravity wave crest. Since the group velocity of capillary waves equals $\frac{3}{2}c$, greater than the phase velocity, the wave energy is propagated upstream of the source, that is on the forward face of the gravity wave, and decays with distance x from the source, while remaining steady in time. If we

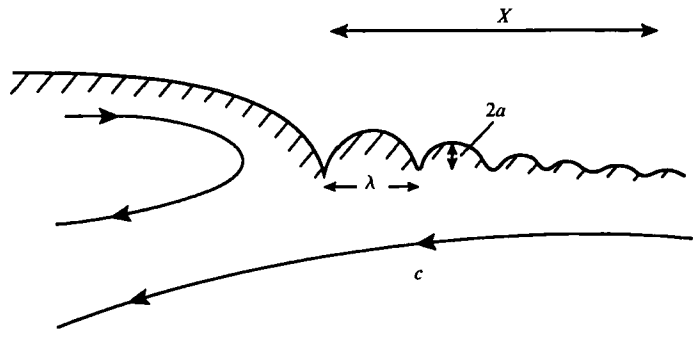

FIGURE 10. Schematic drawing of a capillary bore, with no separation of the flow.

neglect the work done by the current against the radiation stress (see Longuet-Higgins 1963) we can determine the horizontal rate of decay by dividing the right-hand side of (7.1) by the group velocity $\frac{3}{2}c$. Hence

$$\frac{1}{a}\frac{\partial a}{\partial x} = -\frac{4}{3}\frac{\nu k^2}{c}. \tag{7.2}$$

Since the mean velocity is proportional to a^2, the effective length of the wave train is therefore

$$X \sim \frac{3c}{8\nu k^2}. \tag{7.3}$$

A stream flowing beneath the wave train with speed $-c$ passes the wave train in a time t of order

$$t = \frac{X}{c} \sim \frac{3}{8\nu k^2}. \tag{7.4}$$

A wave train of initial steepness $(ak)_0$ at $x = 0$ will, over the decay distance X, have a mean-squared amplitude

$$(1-\mathrm{e}^{-1})\,(ak_0)^2 = 0.632(ak)_0^2. \tag{7.5}$$

We can estimate the magnitude of the vorticity $\bar{\omega}$ shed into the stream by supposing that it is comparable to the total vorticity shed by a uniform wave train of mean-square steepness given by (7.5), over a time t given by (7.4). Thus in (6.6) we write

$$\omega_\infty = -1.264(ak)_0^2\sigma \tag{7.6}$$

and $t = 3/(8\nu k^2)$. This gives

$$\bar{u}_0 = 2.53\left(\frac{3}{8\pi}\right)^{\frac{1}{2}}(ak)_0^2\frac{\sigma}{k} = 0.87(ak)_0^2 c. \tag{7.7}$$

Now we saw in §3, table 1 (and from figure 3), that $(ak)_0$ can be of order 1 so that $\bar{u}_0$, by (7.7), is of the same order as c. In other words, the vorticity generated beneath the capillary waves appears quite capable of generating the velocity differences above and below the roller, even in the absence of wind.

In the case of rollers on a short gravity wave, the velocity difference between top and bottom of the roller is further augmented by the vertical gradient of the orbital velocity in the gravity wave. In addition, work is done on the parasitic capillaries by the orbital motion in the gravity wave (Longuet-Higgins 1963; Longuet-Higgins &

Stewart 1964), causing them to become both shorter and steeper, thus increasing the vorticity that is shed.

8. Vorticity and mass transport

The above conclusions are corroborated by considering the creation of vorticity from the point of view of the capillary wave momentum.

The total horizontal momentum density I in a surface wave on deep water is given

$$I = 2KE/c \tag{8.1}$$

where KE is the kinetic energy density (see for example Longuet-Higgins 1975). For a pure capillary wave (§3) Hogan (1979) has shown that

$$KE = \frac{2T}{\sinh 4\psi_0} \tag{8.2}$$

(since $A = \mathrm{e}^{-2\psi_0}$), while the phase speed c, in dimensional units, is given by

$$c^2 = kT \tanh 2\psi_0 \tag{8.3}$$

(see (3.6)). With equation (8.1) this yields

$$I = \frac{2(T/k)^{\frac{1}{2}}}{(\cosh 2\psi_0)^{\frac{1}{2}} (\sinh 2\psi_0)^{\frac{3}{2}}}. \tag{8.4}$$

For small wave steepnesses ($\mathrm{e}^{\psi_0} \gg 1$) this reduces to

$$I = \tfrac{1}{2}(ak)^2 (T/k)^{\frac{1}{2}}, \tag{8.5}$$

and for the maximum wave steepness $ak = 2.293$, when $\sinh 2\psi_0 = 0.8724$ (from (3.4)), we have

$$I = 2.131(T/k)^{\frac{1}{2}} \tag{8.6}$$

whereas the formula (8.5) would give instead a factor 2.628.

When the capillary wave is damped out by viscosity, the wave momentum I is converted mainly to a horizontal current (though some may go to produce a depression of the mean surface level). By equation (6.3), the depth z to which the momentum is diffused is of order $(\nu t)^{\frac{1}{2}}$ where t is given by (7.4). Thus we have

$$z \sim (\tfrac{3}{8})^{\frac{1}{2}} k^{-1}. \tag{8.7}$$

The mean current velocity is of order I/z. Using (7.4) we have

$$u_0 \sim \tfrac{1}{2}(ak)^2 (\tfrac{8}{3})^{\frac{1}{2}} c = 0.82(ak)^2 c \tag{8.8}$$

in rough agreement with (7.7).

If the capillary waves were dissipated instantaneously by internal friction, the profile of the horizontal momentum would presumably be given by the mass-transport velocity U in the original wave. In figure 11 we show U/c, calculated from

$$\frac{U}{c} = 1 - \frac{T_{\mathrm{E}}}{T_{\mathrm{L}}}, \tag{8.9}$$

where T_{L} is the Lagrangian time

$$T_{\mathrm{L}} = \int \frac{\mathrm{d}s}{q} = \int \frac{\mathrm{d}\phi}{q^2} \tag{8.10}$$

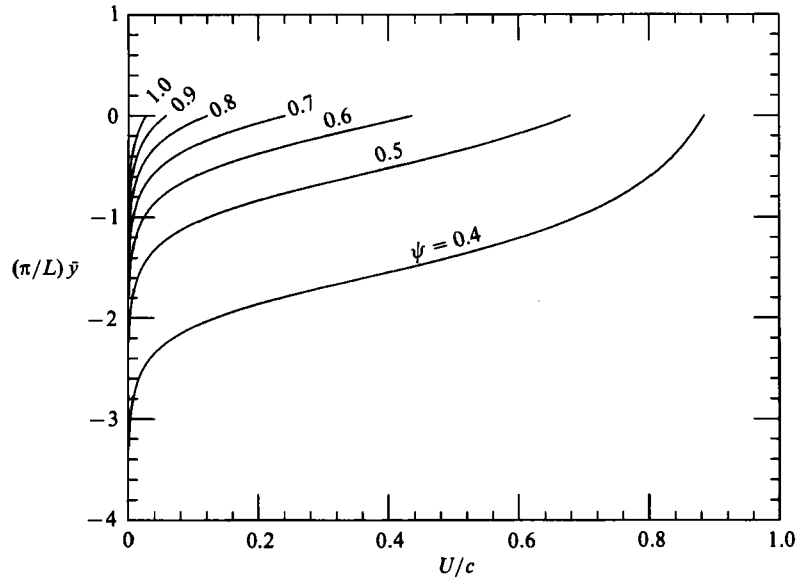

FIGURE 11. The mass-transport velocity U for pure capillary waves, shown as a function of the mean depth $\bar{y}$ of each streamline in figure 5.

integrated along a streamline of the flow in figure 5, and T_E is the Eulerian period $\pi/c = \pi$. This is plotted as a function of the mean depth $\bar{y}$ of a streamline below the mean surface level y_0, for waves of various steepnesses ak. It is notable that for the steepest waves, U/c is close to unity over an appreciable thickness of fluid nearest the free surface. This reflects the fact that the fluid in the rounded crests of the wave all travels forward with nearly the phase speed c. The momentum of this fluid has only to be released into a configuration where the surface is flattened in order to create a positive current moving very nearly with speed c.

9. Steep capillary waves

In very steep capillary waves having sharply curved troughs, such as shown in figures 5(*d*) and 7(*b*), it seems inevitable that the streamlines will separate at the wave troughs. The high vorticity $-2\kappa q$ generated at a trough will give rise directly to a free streamline as in figure 12. The initial velocity difference Δu across the layer will be of the same order as the vorticity ω integrated round the sharp bend, that is

$$\Delta u \sim \int \omega \, \mathrm{d}s = \int (-2\kappa q) \, \mathrm{d}s. \tag{9.1}$$

Since

$$\int \kappa \, \mathrm{d}s = \Delta\theta = \pi \tag{9.2}$$

we see that velocity differences of the same order as q or c are to be expected.

The enclosed space, or 'bubble', in the trough of the limiting wave in figure 5 has long suggested that bubbles of air may be trapped by such waves (see Crapper 1957; Schooley 1958). This no doubt explains the injection of air bubbles beneath capillary–gravity waves as seen in the laboratory by Toba (1961), Koga (1982) and others, although we may also expect the density and viscosity of the air to be of significance in this process.

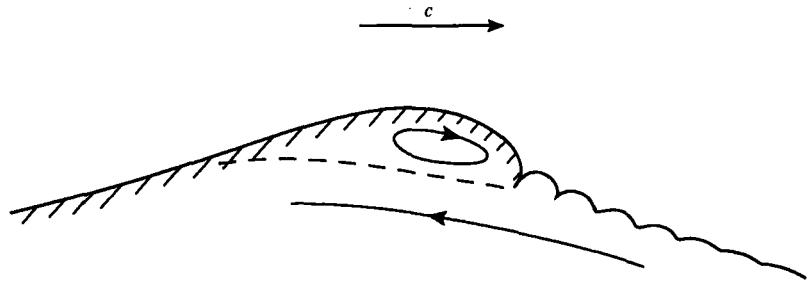

FIGURE 12. Schematic drawing of a crest roller, with flow separation and free shear layer.

We recall that this limiting form of steep waves, in which adjacent wave crests come into contact and trap air, is not confined to pure capillary waves, but is found over a whole range of the parameter (Tk^2/g), as shown by Schwartz & Vanden-Broeck (1979), Chen & Saffman (1979, 1980) and Hogan (1980, 1981). The range of (Tk^2/g) extends even to zero, to include capillary–gravity waves of solitary type on deep water (Longuet-Higgins 1989). Boundary-layer calculations similar to those that we have carried out for pure capillary waves could equally well be performed for all such waves.

10. The development of rollers and bores

The development of a capillary roller at the crest of a short gravity wave appears to be a consequence of the existence of the parasitic capillaries. This in turn may be a phenomenon of irrotational flow, in the first place.

For example, we know the theoretical form of the wave crest in a steep gravity wave (the 'almost-highest wave') as the limiting 120° corner flow is approached (see Longuet-Higgins & Fox 1976). At 'infinity' the flow approaches asymptotically the 120° corner flow, and the only scale length in this solution is the radius of curvature at the crest.

The corresponding irrotational solution including capillarity has not yet been calculated, but we may conjecture that it will feature capillary waves ahead of the gravity wave crest. These must have a speed which enables them to propagate against the backward flow. The source of the capillary wave energy is presumably connected with nonlinear features of the flow near the gravity wave crests, where the lengthscale of the flow is comparable to the wavelength of the capillaries. A first theory for such parasitic capillaries was given by Longuet-Higgins (1963). This assumed the wave amplitude to be due to the perturbation in the pressure brought about by capillarity in the neighbourhood of the gravity wave crest, where the curvature is relatively large. The theory was further developed by Vanden-Broeck (1960) and Crapper (1970), with qualitative experimental confirmation by Chang, Wagner & Yuen (1978) and Yermakoo *et al.* (1986); see also Ebuchi *et al.* (1987). Ruvinsky & Freidman (1981, 1985) and Ruvinsky *et al.* (1991) have developed a theory which takes fuller account of the dynamics of the wave crest, and includes the damping of the capillaries, to first order, but ignores the existence of the roller at the crest.

Gravity waves in a random sea being essentially transitory, steep or breaking waves may appear through wave grouping, in a short time of the order of one wave period. The wave crests may initially be irrotational, or relatively so. However, very soon after the first appearance of the parasitic capillaries, the shed velocity will begin

to build up a vortex at the gravity wave crest. This vortex will tend to accentuate the curvature immediately behind (i.e. downstream of) the first capillary wave, and so increase its amplitude. The dissipation of energy may also reduce the steepness of the gravity wave. But it seems likely that, over a short time at least, there is a positive feedback between the crest roller and the parasitic capillaries. In other words, the configuration of roller and capillaries is self-sustaining, the energy for the flow being drawn from the much larger energy of the gravity wave. A schematic picture is shown in figure 12.

The flow may break down in various ways. One is by dissipation of the energy of the gravity wave (see Longuet-Higgins 1963, §10), or the gravity wave may flatten by the familiar process of moving forwards through a wave group. A second possibility is for the capillary waves to trap air bubbles in the sharp wave troughs as observed by Koga (1982). This process is accompanied by a characteristic circulation near the gravity wave crest, a partial model for which has been suggested by Longuet-Higgins (1990).

A third possibility, which is always present when a laminar viscous flow is pushed to larger Reynolds numbers, is that the flow will pass via instability into a turbulent flow. In such a case the vorticity generated by the capillaries may be replaced entirely by an unstable shear layer between the roller and the underlying flow, and then the parasitic capillaries may disappear altogether. This appears to have happened in the microbreaker shown for example by Banner & Cato (1988); see also Banner & Phillips (1974).

11. Conclusions and suggestions

We have shown that the mean vorticity shed from parasitic capillaries on the forward face of a short gravity wave may contribute substantially towards the vorticity in the roller at the gravity wave crest. Under some circumstances, in the absence of wind, this mechanism may account for all the observed vorticity.

The crest roller and the train of parasitic capillaries form a cooperative system, each sustaining the other. The capillaries may become so steep as to trap air bubbles beneath the surface, as seen by Koga (1982).

The scale of the phenomenon is limited. At larger Reynolds numbers the capillary wave train disappears and is replaced by an unstable shear layer between the roller and the fluid beneath.

At small scales, the role of surface tension and viscosity are all-important. In this paper we have estimated the effect of viscosity in a somewhat *ad hoc* way, as a perturbation to an otherwise irrotational flow. Ultimately, a more radical approach is needed, incorporating viscous boundary conditions from the start.

We have considered the dynamics of the boundary layer mainly from the point of view of vorticity. It may also be fruitful to consider the balance of tangential momentum in the layer (Longuet-Higgins 1969*a*; Csanady 1985), especially over a wavelength of the gravity wave. The generation of mean vorticity $\bar{\omega}_\infty$ by the parasitic capillaries is equivalent in its effects to applying a tangential stress $-\mu\bar{\omega}_\infty$ at the surface of the gravity wave. This tends to pile up an additional mass of fluid lagging 90° behind the applied stress (see Longuet-Higgins 1969*a*). Since the capillaries are on the forward face of the wave, we expect the additional mass to appear near the crest, as is observed. The virtual tangential stress will also contain a second harmonic which will in general cause the gravity wave to become asymmetric, in the horizontal sense. Ordinary, second-harmonic viscous damping

will of course have a similar effect, but the effect of dissipation by the capillaries is much stronger. In fact it may lead to a kind of dissipative coupling between the gravity wave and its second and higher harmonics.

In this paper the direct effect of the wind in producing vorticity at the gravity wave crest has not been discussed, but the following argument suggests that it is small. For, the total horizontal wind stress, which includes the normal pressure fluctuations, is of order

$$\tau_{\text{wind}} = 0.002\rho_{\text{air}} W^2, \tag{11.1}$$

where W is the wind speed. On the other hand by (5.13) the capillaries exert a virtual stress

$$\tau_{\text{cap}} = 2(ak)^2 \mu\sigma \tag{11.2}$$

(cf. Longuet-Higgins 1960, §6). Thus when (ak) is of order 1 we have

$$\tau_{\text{wind}}/\tau_{\text{cap}} = O[10^{-4}(W/c)^2(c^2/\sigma)]. \tag{11.3}$$

where c and σ are in c.g.s. units. But for gravity–capillary waves near the minimum phase speed

$$c^2/\sigma = (2Tg)^{\frac{1}{2}} \approx 200 \text{ dyne/cm}. \tag{11.4}$$

Hence $\tau_{\text{wind}}/\tau_{\text{cap}}$ is of order 0.02 $(W/c)^2$. Since W/c is usually of order 1, the ratio (11.3) is small, reflecting the fact that the capillary wave stress acts over only a small fraction of the wavelength of the gravity waves. Such a localized stress produces, as we have seen, a localized distribution of vorticity.

This work has been supported by the Office of Naval Research under grant no. N00014-91-J-1582.

REFERENCES

BANNER, M. L. & CATO, D. 1988 Physical mechanisms of noise generation by breaking waves – a laboratory study. In *Sea Surface Sound* (ed. B. R. Kerman), pp. 429–436. Kluwer, 639 pp.

BANNER, M. L. & PHILLIPS, O. M. 1974 On the incipient breaking of small scale waves. *J. Fluid Mech.* **77**, 825–842.

CHANG, J. H., WAGNER, R. N. & YUEN, H. C. 1978 Measurement of high frequency capillary waves on steep gravity waves. *J. Fluid Mech.* **86**, 401–413.

CHEN, B. & SAFFMAN, P. G. 1979 Steady gravity–capillary waves on deep water – I. Weakly nonlinear waves. *Stud. Appl. Maths* **60**, 183–210.

CHEN, B. & SAFFMAN, P. G. 1980 Steady gravity–capillary waves on deep water – II. Numerical results for finite amplitude. *Stud. Appl. Maths* **62**, 95–111.

COX, C. S. 1958 Measurements of slopes of high-frequency wind waves. *J. Mar. Res.* **16**, 199–225.

CRAPPER, G. D. 1957 An exact solution for progressive capillary waves of arbitrary amplitude. *J. Fluid Mech.* **2**, 532–540.

CRAPPER, G. D. 1970 Non-linear capillary waves generated by steep gravity waves. *J. Fluid Mech.* **40**, 149–159.

CSANADY, G. T. 1985 Air–sea momentum transfer by means of short-crested wavelets. *J. Phys. Oceanogr.* **15**, 1486–1501.

EBUCHI, N., KAWAMURA, H. & TOBA, Y. 1987 Fine structure of laboratory wind-wave surfaces studied using an optical method. *Boundary-Layer Met.* **39**, 133–151.

HOGAN, S. J. 1979 Some effects of surface tension on steep water waves. *J. Fluid Mech.* **91**, 167–180.

HOGAN, S. J. 1980 Some effects tension on steep water waves. Part 2. *J. Fluid Mech.* **96**, 417–445.

HOGAN, S. J. 1981 Some effects of surface tension on steep water waves. Part 3. *J. Fluid Mech.* **110**, 381–410.

KINNERSLEY, W. 1976 Exact large amplitude capillary waves on sheets of fluid. *J. Fluid Mech.* **77**, 229–241.

KOGA, M. 1982 Bubble entrainment in breaking wind waves. *Tellus* **34**, 481–489.

LAMB, H. 1932 *Hydrodynamics*, 6th edn. Cambridge University Press, 738 pp.

LONGUET-HIGGINS, M. S. 1953 Mass transport in water waves. *Phil. Trans. R. Soc. Lond.* A**245**, 535–581.

LONGUET-HIGGINS, M. S. 1960 Mass-transport in the boundary-layer at a free oscillating surface. *J. Fluid Mech.* **8**, 293–306.

LONGUET-HIGGINS, M. S. 1963 The generation of capillary waves by steep gravity waves. *J. Fluid Mech.* **16**, 138–159.

LONGUET-HIGGINS, M. S. 1969*a* Action of a variable stress at the surface of water waves. *Phys. Fluids* **12**, 737–740.

LONGUET-HIGGINS, M. S. 1969*b* A nonlinear mechanism for the generation of sea waves. *Proc. R. Soc. Lond.* A**311**, 371–389.

LONGUET-HIGGINS, M. S. 1975 Integral properties of periodic gravity waves of finite amplitude. *Proc. R. Soc. Lond.* A**347**, 311–328.

LONGUET-HIGGINS, M. S. 1988 Limiting forms for capillary–gravity waves. *J. Fluid Mech.* **194**, 351–375.

LONGUET-HIGGINS, M. S. 1989 Capillary–gravity waves of solitary type on deep water. *J. Fluid Mech.* **200**, 451–470.

LONGUET-HIGGINS, M. S. 1990 Flow separation near the crests of short gravity waves. *J. Phys. Oceanogr.* **20**, 595–599.

LONGUET-HIGGINS, M. S. 1992 Theory of weakly damped Stokes waves: a new formulation and its physical interpretation. *J. Fluid Mech.* **235**, 319–324.

LONGUET-HIGGINS, M. S. & FOX, M. J. H. 1976 Theory of the almost-highest wave: the inner solution. *J. Fluid Mech.* **80**, 721–741.

LONGUET-HIGGINS, M. S. & STEWART, R. W. 1964 Radiation stresses in water waves; a physical discussion with applications. *Deep-Sea Res.* **11**, 529–562.

OKUDA, K., KAWAI, S. & TOBA, Y. 1977 Measurements of skin friction distribution along the surface of wind waves. *J. Oceanogr. Soc. Japan* **33**, 190–198.

RAYLEIGH, LORD 1890 On the tension of water-surfaces, clean and contaminated, investigated by the method of ripples. *Phil. Mag.* **30**, 386 (Collected Papers, vol. 3, p. 394). Cambridge University Press.

RUVINSKY, K. D., FELDSTEIN, F. I. & FREIDMAN, G. I. 1991 Numerical simulation of the quasi-stationary stage of ripple excitation by steep gravity–capillary waves. *J. Fluid Mech.* **230**, 339–353.

RUVINSKY, K. D. & FREIDMAN, G. I. 1981 The generation of capillary–gravity waves by steep gravity waves. *Izv. Atmos. Ocean Phys.* **17**, 548–553.

RUVINSKY, K. D. & FREIDMAN, G. I. 1985 Improvement of first Stokes method for the investigation of finite-amplitude potential gravity–capillary waves. In *IX All-Union Symp. on Diffraction and Propagation Waves, Tbilisi: Theses of Reports.* vol. 2, pp. 22–25.

SCHOOLEY, A. H. 1958 Profiles of wind-created water waves in the capillary–gravity transition region. *J. Mar. Res.* **16**, 100–108.

SCHWARTZ, L. W. & VANDEN-BROECK, J.-M. 1979 Numerical solution of the exact equations for capillary–gravity waves. *J. Fluid Mech.* **95**, 119–139.

TOBA, Y. 1961 Drop production by bursting of air bubbles on the sea surface. III. Study by use of a wind flume. *Mem. Coll. Sci: Univ. Kyoto* A**29**, 313–343.

VANDEN-BROECK, J.-M. 1960 Mécanique de vagues de grande amplitude. Mémoire pour grade d'Ingénieur Physicien. University of Liege.

WILTON, J. R. 1915 On ripples. *Phil. Mag.* **29**, 688–700.

YERMAKOV, S. A., RUVINSKY, K. D., SALASHIN, S. G. & FREIDMAN, G. I. 1986 Experimental investigation of the generation of capillary–gravity ripples by strongly nonlinear waves on the surface of a deep fluid. *Izv. Atmos. Ocean Phys.* **22**, 835–842.